Atmospheric Research 97 (2010) 129–143

Contents lists available at ScienceDirect

Atmospheric Research

journal homepage: www.elsevier.com/locate/atmos

Calibration of Local Area Weather Radar—Identifying significant factors affecting the calibration

Lisbeth Pedersen [a,b,*], Niels Einar Jensen [a], Henrik Madsen [b]

[a] DHI, Gustav Wieds Vej 10, DK-8000 Aarhus, Denmark
[b] Department of Informatics and Mathematical Modelling, Technical University, Denmark, Building 321, 2800 Lyngby, Denmark

ARTICLE INFO

Article history:
Received 23 June 2009
Received in revised form 13 March 2010
Accepted 15 March 2010

Keywords:
Local Area Weather Radar
Calibration
Z–R relationship
Spatial variability
Precipitation
Uncertainties
Rainfall
Weather radar

ABSTRACT

A Local Area Weather Radar (LAWR) is an X-band weather radar developed to meet the needs of high resolution rainfall data for hydrological applications. The LAWR system and data processing methods are reviewed in the first part of this paper, while the second part of the paper focuses on calibration. The data processing for handling the partial beam filling issue was found to be essential to the calibration. LAWR uses a different calibration process compared to conventional weather radars, which use a power-law relationship between reflectivity and rainfall rate. Instead LAWR uses a linear relationship of reflectivity and rainfall rate as result of the log transformation carried out by the logarithmic receiver as opposed to the linear receiver of conventional weather radars. Based on rain gauge data for a five month period from a dense network of nine gauges within a 500×500 m area and data from a nearby LAWR, the existing calibration method was tested and two new methods were developed. The three calibration methods were verified with three external gauges placed in different locations. It can be concluded that the LAWR calibration uncertainties can be reduced by 50% in two out of three cases when the calibration is based on a factorized 3 parameter linear model instead of a single parameter linear model.

1. Introduction

Rainfall forecasting has always been strongly desired by hydrologists as it provides time for preparation, thereby facilitating damage control and making it possible to optimize treatment plants prior to a rainfall event. Hydrologists operate at a wide range of scales in time and space, from small urban catchments with a response time of minutes and hours, to large rural watersheds where the response scale is hours or even days. Today urban areas are spreading in most parts of the world. This leads to new challenges for urban drainage systems as new developments often have to be connected to the existing system of sewers and waste water treatment plants (WWTP). The design of the existing systems is most often based on a set of Intensity Duration Frequency (IDF) curves derived from regional historic rainfall records, i.e. based on rain gauge measurements. As a result of the use of historic rainfall data for the design, existing sewer systems are not designed for a potential increase in rainfall amounts as well as increase in the frequency of more extreme rainfall resulting from climate changes (Mailhot et al., 2007; Grum et al, 2006; Arnbjerg-Nielsen, 2006).

Hydrologists, urban planners and scientists are working in a range of areas to meet the challenges in urban drainage connected to climate changes and increased urbanization. The simple approach is to increase the dimension of the pipes, but in most cases this is an extremely expensive solution and in some cases not a realistic one due to practical and economical reasons. Constructing detention basins, two-string sewer systems, water harvesting facilities, local percolation facilities and other initiatives for surface water are all solutions being looked upon and also implemented in many places these years (Chocat et al, 2001). An option is to utilize the existing sewer system in a more optimal way by

* Corresponding author. DHI, Gustav Wieds Vej 10, DK-8000 Aarhus, Denmark. Tel.: +45 8620 5116.
E-mail address: lpe@dhigroup.com (L. Pedersen).

0169-8095/$ – see front matter © 2010 Elsevier B.V. All rights reserved.
doi:10.1016/j.atmosres.2010.03.016

real-time control (RTC), enabling water volumes to be detained in some areas or to be de-routed in order to increase the capacity in other areas. It thereby becomes possible to increase the effective system volume, to reduce sewer overflows and to optimize the constituent part of water being treated by the WWTP. Such an integrated real-time control project is currently being implemented by Aarhus Water in Aarhus (pop. 306,000), Denmark.

RTC requires online information from sensors in the sewer system, e.g. water levels, pumping data or flow in critical points that is transmitted to a central place where either software or humans take action. The problem with this is that these sensor types only provide information on increased flow after the rainfall has reached the system, where the real advantage would be to get the information in advance so that the system could be optimized beforehand. This requires a detailed accurate forecast of the rainfall with a spatial and temporal resolution in the same domain as the sub catchments. Rain gauges are insufficient in this connection as they are point measurements. Furthermore there will often not be enough of them meaning that they often miss the peak intensities (Einfalt et al., 2005). Weather radars on the other hand are capable of providing spatially distributed information on rainfall over large areas. Radars can provide data for forecasting future rain over the catchments with up to a few hours of lead time. Like rain gauges, weather radars have shortcomings, since the radar rainfall estimate is an indirect measurement of the rainfall and requires input from a gauge or disdrometer for calibration and the uncertainty of the estimate is increasing with range (Battan, 1973; Zawadzki, 1984).

In 1999 the EU project ESPRIT 23475 “High Performance Rainfall Radar Image Processing for Sewer Systems Control” was completed. The aim of the project was to utilize existing C-band radars to provide detailed forecasts for RTC of sewers. Since data from one of the pre-appointed existing radars were unavailable in real time, it was decided to develop a high resolution cost-efficient weather radar capable of providing detailed forecasts of rainfall for urban areas. The result was the Local Area Weather Radar (LAWR) based on an X-band marine radar. Partners in the LAWR development were DHI and the Danish Meteorological Institute (DMI), and today the LAWR is manufactured by DHI.

Conventional weather radars such as S-band and C-band are poor at detecting near surface phenomena at long ranges since the beam height above the surface is increasing with range due to the curvature of the earth. In addition to this the spatial resolution of conventional weather radars is often 1–16 km^2 which is high when compared to e.g. urban catchment sizes which can be as small as one tenth of the pixel sizes or less. The weaknesses mentioned here have resulted in strong focus on the use of X-band radars for meteorological purposes over the past few years. There are several groups around the world working on using X-band radars for meteorological applications both for research purposes and for commercial purposes. The Collaborative Adaptive Sensing of the Atmosphere (CASA) project is one of the largest of these groups working towards creating a distributed network of low-cost, low-power solid state radars with Doppler, dual-polarization capabilities covering the United States (Brotzge et al., 2006; Donovan et al., 2006) and sources herein. Beside the LAWR made by DHI, several other commercial X-band weather radar systems exist, e.g. the HYDRIX by Novimet (Bouar et al., 2005) and the RainScanner from Germatronic (Gekat et al., 2008). Overall they share the X-band characteristic such as a 3.2 cm wavelength, but differ in a number of areas with regard to specifications such as antenna type (dish vs. fan beam), receiver, Doppler capability, spatial and temporal resolution of output, range and price.

The LAWR being an X-band radar differs on a number of features compared to standard C-band and S-band weather radars, and it also uses a different calibration method. The primary differences between the radar types are: wavelengths (~3 cm for X-band, ~5 cm for C-band and ~10 cm for S-band), peak power (25 kW for X-band, 250 kW for C-band, 700 kW for S-band), antenna size and design, logarithmic (C-band, S-band) vs. linear receiver (LAWR) and finally there is a significant difference in cost — the X-band technology is more cost-efficient than the C-band and S-band technology. The figures here can vary for individual radar installations that have been customized.

This paper focuses on evaluation of the LAWR calibration method and the uncertainty of LAWR rainfall estimation. The work is state of the art as it is the first full evaluation of the LAWR calibration method using standard tipping bucket gauges and incorporating uncertainty of using as single gauge to represent a radar pixel area of 500×500 m. Focus is on identification of parameters contributing to the calibration along with uncertainties related to the spatial variability of rainfall. The evaluation is based on experimental data. The uncertainties related to spatial variability of rainfall within a pixel will be present in any radar calibration and are of great significance as these uncertainties will be added to those of the application using radar data as input.

2. Local Area Weather System

The LAWR is based on a 25 kW X-band marine radar manufactured by Furuno. The characteristics of the LAWR are listed in Table 1. The LAWR is not equipped with doppler or dual-polarization technologies.

The marine radar is designed to operate continuously in harsh conditions at sea thereby reducing maintenance requirements. Only the magnetron needs to be changed every 8 months. The LAWR system is designed to use the raw

Table 1
System data for the LAWR system.

	LAWR
Peak power	25 kW
Wave length	X-band 3.2 cm
Pulse length	1.2 μs
Antenna	2.5 m slotted waveguide array
Receiver	Logarithmic receiver
Vertical opening angle	±10°
Horizontal opening angle	0.96°
Samples pr. rotation	360
Range (forecast/QPE)	60/20 km
Spatial resolution	500×500 m
	250×250 m
	100×100 m
Data output frequency	1 or 5 min
Scanning strategy	Single layer and continuous scanning

video signal without any modifications of the original Furuno antenna unit thereby limiting vulnerability issues. The analog raw video signal ranges from 0 to −9 V and is converted to a 10 bit digital signal ranging from 0 to 1024 by the custom-made A/D converter sampling with 20 MHz. Originally the video signal was set to range from 0 to −6 V by the manufacturer, and the signal processing was adapted to this range. It was later discovered that the signal range was wider, and subsequently an adjustment box tuning the signal to the range of the A/D converter was implemented in the system, cf. Fig. 1. The system consists of the antenna unit, the transceiver, a custom-made 20 MHz A/D converter, two standard PCs and a monitor. The system is designed to run automatically and can be operated from afar. An overview of the system and optional features is shown in Fig. 1.

2.1. Scanning strategy

Conventional weather radars operate with a range of scanning strategies depending on their type and on their operational purposes, however, the majority of radars share the feature that they scan one full 360° circle at each elevation angle before tilting the antenna to the next elevation angle. This has the effect that a given point only is scanned/observed once at each elevation. The scanning cycle normally takes from 5 to 15 min, causing timing issues due to the velocity of the rainfall field combined with the spatial variability of the rainfall changing over time. This needs to be dealt with carefully when processing data, especially when creating 2D surface rainfall maps such as CAPPI (Constant-Altitude Plan Position Indicator) products in order to avoid timing issues when applications use the radar data as input (Rinehart, 2004; Doviak and Zrnic, 2006).

The LAWR uses an alternative scanning strategy. It scans continuously with 24 rpm with a horizontal opening angle of 0.96° resulting in 360 scans in each rotation. The temporal resolution is chosen by the user to be either 1 or 5 min, so the estimation of rainfall at a given point at the surface is the average of 24 or 120 data samples of that point. The number one shortcoming of the LAWR is the large vertical opening angle of ±10°. Only the upper half of the ±10° is used since the lower half is cut-off either by nearby obstacles or by a mechanical clutter fence. With a vertical opening angle of 10°, the sample volume increases rapidly with range, and at a range of 20 km the beam is 3.5 km high and at 60 km it is 10.5 km high. The maximum range of 60 km is limited compared to the maximum range of 240 km of conventional weather radars, however, the problems with overshooting near surface phenomena at far ranges is eliminated as a result of the short range. The cost of X-band technology compared to C-band, or the even more expensive S-band, is lower so it is possible to install a number of X-band radars to cover the same area covered by a C-/S-band radar for the price of one of these.

2.2. Signal processing

Signal processing from backscattered energy to data files can be broken down into four parts: Reception, A/D converting, data processing and data storage. The primary part of signal processing is done by the Signal Processor PC, cf. Fig. 1 where the digitalized voltage signal is processed into reflectivity values. Every minute, 120 megabytes of raw data is processed by the Signal Processor PC, and at the end of each scanning cycle (1 or 5 min) the 120/600 megabytes of data is pushed to the Communicator PC for final processing and data storage. During the data collection, the data is applied to a number of schemes in order to handle well-known radar obstacles e.g. clutter and attenuation. Because it is an X-band radar, the LAWR is of course sensitive to attenuation due to the wavelength of 3.2 cm, but as part of the signal processing, the data is corrected for attenuation. The attenuation

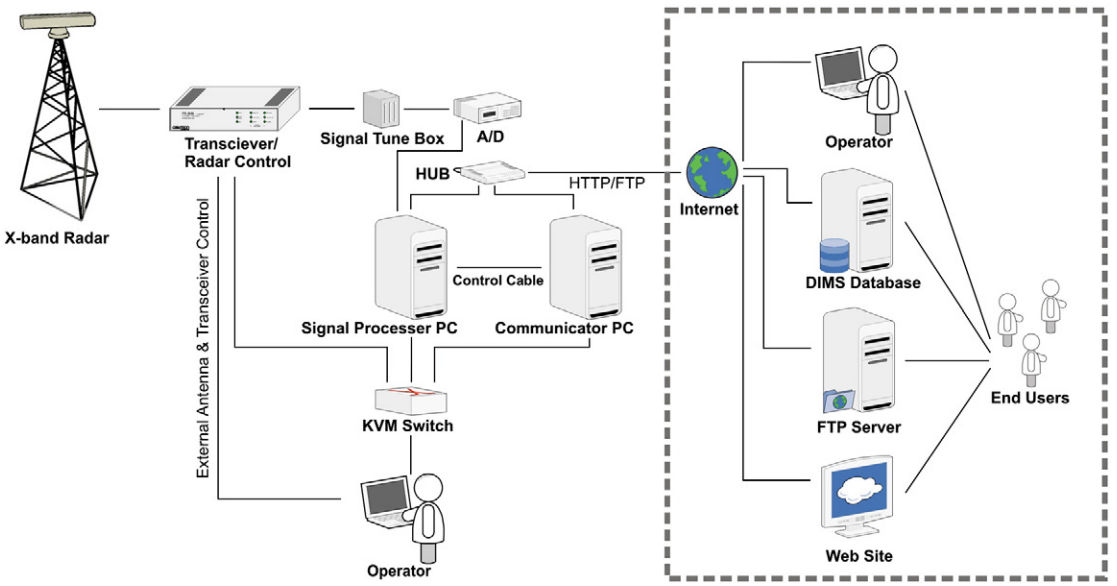

Fig. 1. System layout of the Local Area Weather Radar. The subjects within the dashed line are optional features all requiring internet access to the LAWR installation. The radar is here illustrated on a mast, but is as often placed on an existing installation such as a rooftop.

correction is applied along the path of each raw scan line. For each sample bin, the adjusted reflectivity, Z_r is estimated as follows:

$$Z_r = Z_{g,r}\left(1 + \frac{\alpha \sum_{i=0}^{r-1} Z_i}{C_1 \cdot n_{samples}}\right) \quad (1)$$

where:

Z_r	adjusted reflectivity value at range r
$Z_{g,r}$	uncorrected reflectivity at range r
$n_{samples}$	number of samples in a single scan line, typical value is 8000
α, C_1	empirical constants where typical values are 1.5 and 200, respectively.

The LAWR attenuation algorithm enhances the signal proportionally to the amount of power used at a given range without changing the properties of the rainfall event when observed from both sides as shown in Fig. 2. If too much correction is applied, the rainfall intensities will be over-enhanced with increasing range from the radar and vice versa in the event of inadequate correction. The method was developed, tested and verified as part of the original LAWR development project.

Furthermore, data is applied a volume correction scheme handling the rapidly increasing sampling volume with range due to the 10° vertical opening angle. If no volume correction scheme is applied, the LAWR will underestimate the rainfall with increasing range, which becomes evident if data is accumulated over a longer period e.g. more than two months. An accumulation period of two months is normally used in Denmark where rainfall is frequent, but in different climate regimes it may be necessary to adjust this period. The accumulated rainfall field is not homogeneous over the area; it peaks in the vicinity of the LAWR and decreases with range. This is due to the fact that at far ranges a higher quantity of rainfall is required in order to pass the noise cut-off threshold value, due to the greater vertical integration length. To compensate for the increasing beam, a volume correction algorithm was developed to compensate for this issue. The method assumes homogeneity of the radar coverage area over an accumulation period of two months. The accumulated LAWR image is subdivided into a number of concentric circles with the radar in the centre, and an exponential function is fitted to the average of each circle using a reference distance of e.g. 5 km. The reference distance is the point where the exponential function is forced to 1. The exponential function outperformed other function types (power law, linear and higher order polynomials) which were tested initially. In order to avoid extreme correction values, a constraint of a maximum correction of 4 is enforced. When the volume correction is applied to the data, the reciprocal of the function is used to adjust for the in-homogeneity as function of range. The applied volume-corrected reflectivity at range r, Z_{rv} is estimated by:

$$Z_{rv} = Z_r \frac{1}{C_2 \cdot exp(r \cdot C_3)} \quad (2)$$

where:

Z_{rv}	volume-corrected reflectivity at range r
Z_r	adjusted reflectivity at range r from Eq. (1)
r	range
C_2, C_3	empirical constants that are location dependent. Initial value estimate: 1 and −0.03.

Until recently the only output format of the LAWR was data in Cartesian coordinates in the resolutions chosen by the user (Table 1), but raw polar data is also available today. The conversion from polar to Cartesian grid is by interpolation, and as a result some of the spatial information is lost. Furthermore, at ranges larger than 1 pixel width (6 km for 100×100 m pixels, 15 km for 250×250 m pixels, 30 km for 500×500 m pixels) the values are interpolated. The LAWR format and data processing was developed so it would be consistent with that used by the radars operated by the Danish Meteorological Institute at the time of development. Therefore a 9 by 9 pixel median filter for removing extreme abnormalities was implemented in the original data processing. In the view of the fact that the work linking extreme value statistics and establishing IDF curves based on LAWR

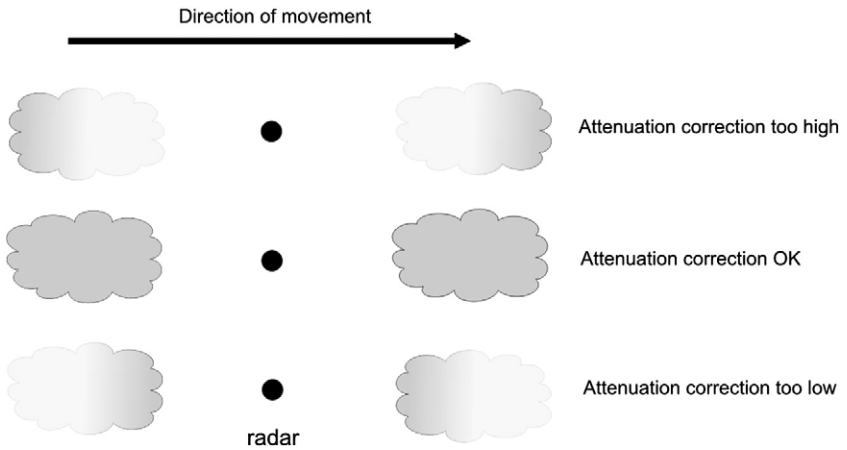

Fig. 2. LAWR attenuation correction principle. The cloud symbolizes a rainfall event observed at two different time steps — before and after passing over the radar. If the applied correction is too powerful the remote part of a rainfall event (as observed from the radar) will be over-enhanced while inadequate correction will result in suppression of the remote areas of the rainfall event.

data are highly sensitive to this option since the median filter removes the peak values which are of interest in this context. Therefore the median filter is not used today in the signal processing.

The output from any radar is not rainfall intensity, but reflectivity, representing the water content in a given radar bin. Radar reflectivity depends on the distribution of drops observed in the sample volume, and the same radar reflectivity value can therefore represent different water contents. In order to use the radar data as a rainfall estimate in the same manner as that observed by a rain gauge, it is therefore necessary to apply a calibration. The LAWR calibration as well as the conventional radar calibration is outlined in the following section.

3. Weather Radar Calibration

One of the first reports of measuring rainfall using a radar was reported by Marshall et al. (1947) who suggested that there is an empirical power-law relationship between the reflectivity factor, Z and the rain rate R of the form $Z = AR^b$ — the so-called Z–R relationship. Marshall et al. (1947) suggested $Z = 190R^{1.72}$ based on experiments with a military radar. One year later Marshall and Palmer published their famous paper "The distribution of raindrops with size" proposing a Z–R relationship of $Z = 220R^{1.60}$ based on raindrop size distributions obtained experimentally (Marshall and Palmer, 1948). The constants of the power law express the distribution of drops in the volume sampled by the radar. The work of Marshall and Palmer (1948) formed the basis for research in the use of weather radars for estimating rainfall, and their approach is still widely used today in an operational context (Lee and Zawadzki, 2005).

In the 60 years that have passed since the early days of weather radars, many things have improved. The introduction of computers for displaying and processing the data is probably the most significant change, but also hardware developments of antenna, transceiver and electrical components have led to significant improvements in terms of stability and accuracy. The implementation of Doppler technology during the late 1980s and 1990s further improved the radar rainfall estimates. The latest addition is dual-polarization technology to the operational weather radar networks around the world. All these developments have reduced some of the uncertainties and added information to the meteorologists and researchers, but nevertheless the focus point is still the conversion from received power backscattered from the rain in the atmosphere to rainfall intensity. Despite enhanced equipment, 60 years of research in weather radars and atmospheric sciences, and new instruments such as the 3D Video disdrometer many still doubt the capabilities of weather radars for rainfall estimation at surface. The number one argument is that rainfall estimation by a weather radar is too uncertain because the comparison with the so-called ground truth, a single rain gauge, shows either over- or underestimation of both rainfall intensities and accumulated rainfall depths over a given area (Austin, 1987; Zawadzki, 1974; Zawadzki, 1984; Einfalt et al., 2005 and sources herein).

The reasons for the discrepancy between gauge and radar rainfall estimates have been widely addressed in the literature for the past 60 years, with primary focus on improving the radar calibration and understanding the uncertainties related to the Z–R relation. It was acknowledged early on that a unique global set of a and b constants does not exist and (Battan, 1973) summarizes 69 different Z–R relationship from various sources worldwide showing a wide range of constants. Since Battan's study large research efforts have been put into understanding the physical properties of the processes of the drop size distribution (DSD), the variability of the DSD and uncertainties since they are related to the Z–R relationship by (Zawadzki, 1974; Ulbrich, 1983; Austin, 1987; Zawadzki, 1984; Ciach and Krajewski, 1999; Jameson and Kostinski, 2001; Uijlenhoet, 2001; Lee and Zawadzki, 2004; Fiser, 2004; Lee and Zawadzki, 2005; Lee et al., 2007; Uijlenhoet et al., 2008) among others. The research continues and the introduction of dual-polarized weather radars has facilitated new ways for estimating parameters describing the DSD (Lee and Zawadzki, 2004). Depsite this, most operational systems use a simple Z–R relationship e.g. $Z = 300R^{1.5}$ or the Marshall Palmer $Z = 200R^{1.6}$ (Lee and Zawadzki, 2005).

The uncertainties related to the radar rainfall estimation are often focused around the DSD variability and the uncertainty related to choosing the right Z–R relation, however, there are several other contributing factors, e.g. hardware system calibration, meteorological phenomena (e.g. bright band), beam interception, timing of sampling just to mention a few. These factors can largely be divided into three groups: Sources of random errors, sources of systematic errors and sources of range dependent errors, even though some factors can be classified as belonging to more than one group (Zawadzki, 1984).

In an analysis comparing radar rainfall estimates with observed rainfall at a given rain gauge station, the uncertainties related to rain gauges are rarely mentioned and hardly ever quantified. The reason for this is probably the general perception of the rain gauge being the ground truth and the discussion of the related uncertainties is of the past. As rain gauges are mechanical devices, they can suffer from instabilities, errors and mis-calibration as any other instrument. On top of this are the uncertainties related to placement, sheltering (can change over time e.g. due to growing trees) and wind-induced errors. In order to obtain reliable rain gauge data, costly regular maintenance and meticulous data control are required in order to avoid flawed data (Krajewski et al., 2003).

In addition to all the uncertainties mentioned above there is the issue of scaling. The fact is that radar rainfall estimates are evaluated based on point measurements. The typical pixel size of conventional weather radars is 1×1 km or 2×2 km whereas the sample area of a rain gauge is typically 200–300 cm^2, which corresponds to comparing the continent of Europe with a radar pixel in terms of difference in the spatial domains. The variability of rainfall within an area as small as a single pixel can be significant and have impact on the radar calibration (Habib and Krajewski, 2001; Krajewski et al., 2003; Pedersen et al., 2010). Furthermore, the radar samples a volume projected onto a 2D surface at a given height above the surface. The sample size increases with range and is an average over the duration of the scanning cycle, whereas the gauge measurement is a discrete measure defined by the

gauge bucket volume. Another factor contributing to the discrepancy between radars and gauges are situations with partial pixel filling. When pixels are 1×1 km or even larger there will be cases where the gauge does not observe rain while the radar does and vice versa. Habib and Krajewski (2001) find that for a 5-minute timescale there is approximately 30% probability that a single gauge does not observe rainfall within an area of 1×1 km and the probability increases to about 50% when the area is 3×3 km. They furthermore state that these probabilities are likely to be conservative since a higher density of gauges could lead to higher values. This is an issue often overlooked in the discussion of radar performance.

3.1. Local Area Weather Radar Calibration

One of the objectives when the LAWR was developed was to make a cost-efficient supplement to rain gauges, and therefore an existing marine X-band radar was chosen. The drawback of this decision is a large vertical opening angle of the beam ($\pm10°$) and a logarithmic receiver which is contrary to the linear receiver of conventional weather radars. The logarithmic receiver in combination with no available disdrometers for the first calibrations led to a search for an alternative method for calibrating the LAWR. The missing disdrometer data would constrain the calibration since it would only be possible to apply literature standard Z–R relations. This would result in added uncertainties in the calibration of the LAWR since the Z–R relationship would have been obtained by a different radar type in a different climate regime.

A preliminary experimental comparison of a LAWR and the Danish Meteorological Institute's C-band radar on Rømø was carried out in 2001 were it was concluded that the LAWR results appeared reasonable compared to those of a C-band radar. The spatial extent of the rainfall areas was well captured, but the intensities, especially the lower ones, were more uncertain (Overgaard, 2001). It should be noted that the comparison only used a very limited number of events and that the LAWR at that time used an early version of the A/D converter with less sensibility. A conversion curve from the LAWR reflectivity to dBZ was established by Overgaard (2001) which made it possible to convert the reflectivity value of the LAWR to a corresponding dBZ and thereby enable the use of a Z–R calibration. A description and example of such a conversion curve can be found in Pedersen (2004). However, a new conversion curve would need to be determined due to the different A/D converter used today.

Different calibration methods have been developed and tested, but common for them all is that they use a black box modeling approach. The output from the LAWR is related directly to the rainfall observed at ground by a rain gauge without any attempt to include physical properties such as a drop size distribution of the rain drops in the sample volume. The reason for pursuing a different approach than the one outlined by Overgaard (2001) is to avoid dependency of a close-by C-band radar for creating the conversion curve required for this type of calibration. The conversion turned out to be a log-transfer function as expected taking the two types of receiver into consideration. The first initial attempts showed an obvious relationship between the LAWR reflectivity and 5-minute integrated rainfall intensities, however, it was found that the resolution of a 0.2 mm tipping bucket rain gauge (Rimco) was too coarse to establish a relationship between the reflectivity and gauge intensity when each 5-minute time step was used. Instead rainfall intensities obtained by an optical drop counting gauge (Pronamic) with a resolution of 0.01 mm were used and a second order polynomial was fitted to the data with a good result (Jensen, 2002).

To test the validity of the second order polynomial relationship and address the uncertainties of using a single gauge for calibrating the LAWR, a field experiment was carried out in 2003. Nine optical drop counting gauges were placed equally representing one ninth of a single LAWR pixel (500×500 m). On the basis of the data from this experiment it was concluded that accumulated rainfall as measured by rain gauges can vary significantly and thereby add uncertainty to the LAWR calibration despite the small pixel size (Pedersen, 2004; Jensen and Pedersen, 2005). The second order polynomial was based on a fit of 5-minute integrated values from both LAWR and gauge. An evaluation of the second order polynomial showed that the relationship was equally well described with a linear relationship, but the method required data from high resolution rain gauges (0.01 mm), which is a lot finer than that of standard tipping bucket rain gauges of 0.1, 0.2 and 0.4 mm. So gauges that were already installed could not be used to calibrate the LAWR. It was then discovered that a strong linear relationship existed between the total sum of LAWR reflectivity and the rainfall depth in mm resulting in the same slope coefficient (calibration factor) as when based on 5-minute values. This discovery facilitated the use of standard 0.2 mm tipping bucket gauges since the total rainfall depth is used instead of intensities. The calibration gives a factor, denoted DHI CF, which when applied to the LAWR output (Z) gives the radar rainfall intensity (Pedersen, 2004):

$$DHI\,CF = \frac{\sum_{Event\,Start}^{Event\,Stop} mm\ rain\ [\text{gauge}]}{\sum_{Event\,Start}^{Event\,Stop} Z/\Delta t\ [\text{LAWR}]} \tag{3}$$

where $Z/\Delta t$ is the output from the LAWR per time step (Δt), which is either 1 or 5 min. The method is used as the standard LAWR calibration method today and is sometimes referred to as the “Sum Calibration Method”.

As mentioned above the relationship between radar rainfall measurements and rainfall at ground is normally described by a power-law function. Jameson and Kostinski (2001) argue that when based on physical considerations, the relationship between Z and R should be linear. The linearity will appear in statistically homogeneous data (mean and variance are independent of the choice of origin), whereas non-linearity appears when statistically inhomogeneous (mean and variance depend on the origin and can thereby change throughout the dataset) data are used. The presence of power laws is explained by the fact that almost all Z–R relations are derived from statistically inhomogeneous dataset, since rainfall is not uniformly distributed but rather clustered (Jameson and Kostinski, 2001). The rainfall observed by the LAWR will in most cases be statistically inhomogeneous, but with the transformation carried out by the logarithmic receiver combined with the arguments from

Jameson and Kostinski (2001) and the existing data analysis there seems reason to believe that the approach is reasonable.

4. Case study

The performance of the LAWR calibration method and the uncertainty of using a single rain gauge for the calibration are addressed with data from a rainfall measuring field campaign. To measure the variability of rainfall within one LAWR pixel of 500 × 500 m nine rain gauges were deployed from 2007 to 2009. The rain gauges were set up to validate the finding based on a similar experiment in 2003 reported by Jensen and Pedersen (2005). The results from the 2007–2009 experiment are reported in Pedersen et al. (2010). For this study data from the Aarhus LAWR has been used, cf. Table 1 for specifications, to assess the LAWR calibration method together with data from the 2007–2009 rain gauge measuring campaign and three validation gauges. The nine gauges are placed so that they each represent one ninth of a LAWR pixel. An overview of the location is illustrated in Fig. 3 along with a close-up of the rain gauge layout. The gauges are located in the water of Norsminde Fjord, a shallow estuary. The area of interest is located around the city of Aarhus, Denmark, and the rain gauge site is at latitude 55°59.4′N and longitude 10°15.8′E.

The misalignment between the gauges and the Aarhus LAWR 500 × 500 m grid in Fig. 3 is due to the fact that at the time when the gauges where commenced, it was believed that the grid was rotated 6° clockwise, however, the grid rotated −5° counter-clockwise instead. The discrepancy was a result of different projections. The result is that all gauges are not within a single pixel in the Cartesian grid format as illustrated in Fig. 3 and listed in Table 2.

4.1. Available data

The gauge dataset consists of 2 seasons of measurements from September–November 2007 and June–November 2008. Only the 2008 dataset is used in the calibration analysis, since the 2007 gauge data was not calibrated in-situ as the 2008 gauge data, and the 2007 radar data was applied to the median filter. Detailed description of the rain gauge experiment, calibration procedures, data control and uncertainties can be found in Pedersen et al. (2010).

During the 6 months of 2008 only 8 rainfall events were recorded by all 9 gauges simultaneously — the vast majority

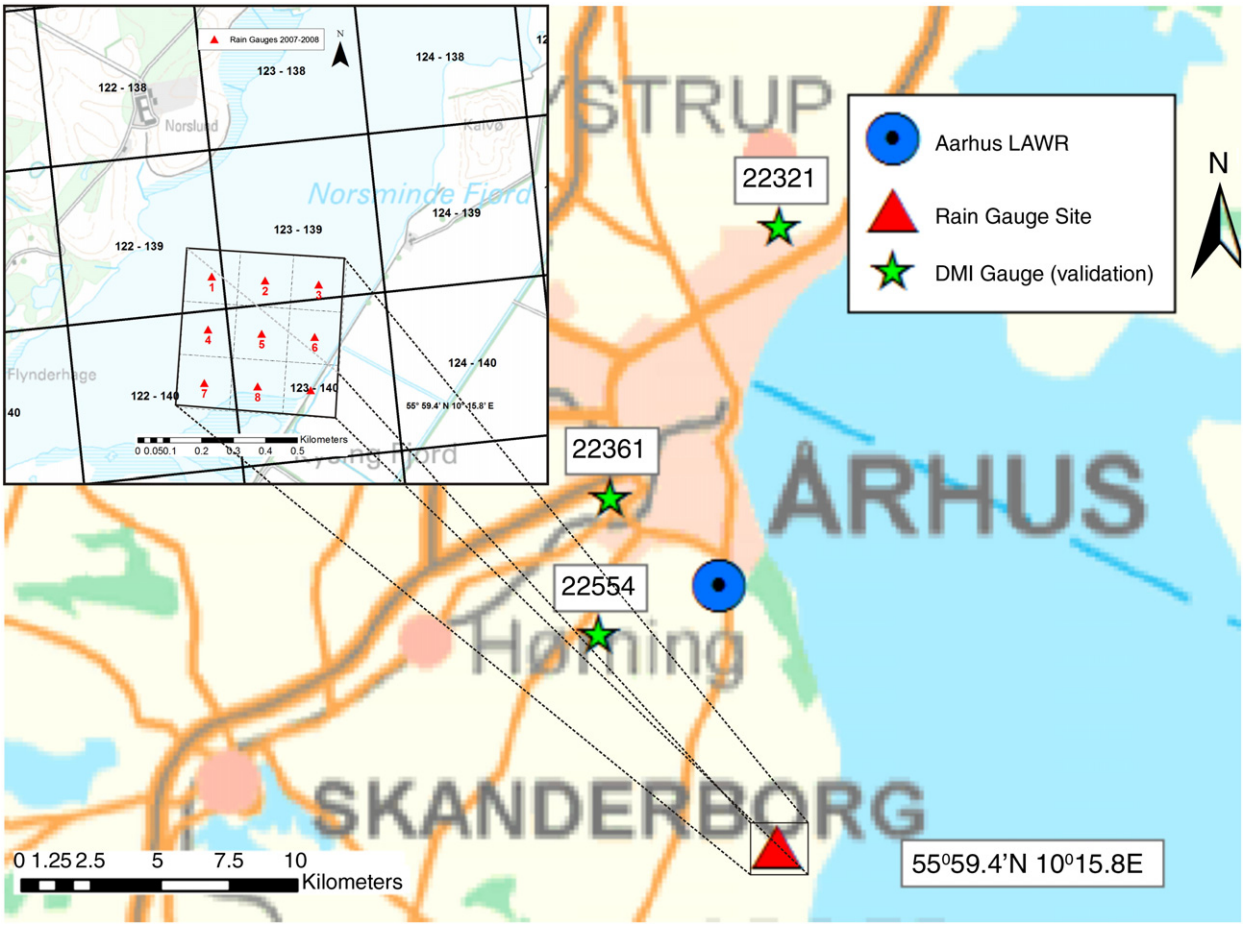

Fig. 3. Overview of area with the LAWR and the rain gauges. The Aarhus LAWR is located just south of Aarhus, Denmark and the rain gauge test site is located at 55°59.4′N and 10°15.8′E. The gauges used for validation is marked with stars and are part of the official rain gauge network in Denmark managed by the Danish Waste Water Pollution Committee (SVK). The inserted picture is a close-up of the rain gauge test site shown in relation to the 500 × 500 m grid of the Aarhus LAWR.

Table 2
Gauges and corresponding pixels in the Cartesian grids of the Aarhus LAWR.

	Gauge type	Distance to Aarhus LAWR [km]	Pixel (col,row) [500×500 m]	Pixel (col,row) [100×100 m]
1	Pronamic	9.3	122,139	160,244
2	Pronamic	9.3	123,139	162,245
3	Pronamic	9.3	123,139	163,245
4	Pronamic	9.8	122,140	160,246
5	Pronamic	9.8	123,140	162,246
6	Pronamic	9.8	123,140	163,247
7	Pronamic	9.8	122,140	160,248
8	Pronamic	9.8	123,140	161,248
9	Pronamic	9.6	123,140	163,248
22554	Rimco [a]	4.9	111,123 [b]	105,163 [b]
22361	Rimco [a]	5.3	113,113	115,115
22321	Rimco [a]	13.3	128,95	186,23

[a] Operated by the Danish Meteorological Institute.
[b] On the border to 112,123/106,163.

of rainfall events were observed by 3–9 gauges, cf. Table 3 for a summary of gauge data. The missing observations are a result of lightning, clogged gauges as a result of bird droppings and brake-downs. Especially Gauge 1 suffered from malfunctioning and only observed 12 rainfall events in total.

The data was collected over 6 months from 17 June to 13 November 2008 and has been divided into individual rainfall events inspired by a method used for the Danish Water Pollution Control Committees network of rain gauges in Denmark operated by the Danish Meteorological Institute (DMI). A rainfall event must consist of at least 2 registrations and the time span between these registrations must be less than 60 minutes (Thomsen, 2007). A requirement of minimum rainfall depth of 1 mm has furthermore been applied. The rainfall depths for the individual rainfall events (55 in total) and the average rainfall event intensity are shown in Fig. 4.

If the reflectivity from a single pixel (number (123,140) — over 4 of the 9 rain gauges) is accumulated over a month and compared with the regional rainfall depths for the Aarhus region reported by the Danish Meteorological Institute based on interpolated rain gauge data from several gauges in the area (DMI, 2008), the overall agreement is good as seen in Fig. 5.

Table 3
Gauge data summary.

Gauge	Number of events>1 mm	Total rainfall depth [mm]	Range rainfall intensity [mm/h]
22554	80	273	0.5–21
22361	74	326	0.5–25
22321	80	242	0.7–42 [a]
1	12	79	0.5–14.3 [b]
2	34	202	0.3–26.9
3	26	149	0.6–26.5
4	50	297	0.3–28.5
5	40	220	0.3–10.8
6	52	286	0.3–28.3
7	41	248	0.4–32.5
8	43	226	0.3–28.1
9	55	295	0.3–26.2
Average of 1–9	39	222	3.6

[a] The maximum intensity of 42 mm/h is a single event where 1.4 mm fell over 2 min. The second largest is 20.3 mm/h.
[b] Gauge 1 suffered seriously from malfunctioning and only observed 12 events in total.

The difference in the spring and early summer months is due to the fact that the magnetron was worn out and needed to be replaced, which was done on 30 June. The state of the magnetron is interpreted based on the average reflectivity value level over the full coverage area. The dry weather value drops when the magnetron is worn out. As result of this, all data prior to the magnetron change have been omitted from the analysis.

The discrepancy in November is probably due to the fact that the precipitation in this period was dominated by low-hanging light rainfall which is not very well observed by the LAWR due to the large beam. To illustrate the problem with shallow precipitation systems, the percentage a given cloud constitutes of the beam is plotted in Fig. 6, where it is seen that low-hanging precipitation only fills a fraction of the beam even at short ranges and thereby results in underestimation of the rainfall intensity.

4.2. Preparation of LAWR data

To compensate for underestimation as a result of increasing beam volume with range, a second volume correction (Eq. (2)) is applied to the data prior to calibration. To accommodate for seasonal changes a new parameter set for the volume correction is estimated for every 10–15 days based on data from the previous 60 days, and a daily value is found by interpolation in cases of post-analysis. The process is part of the automatic calibration module running on some LAWR systems and here a new parameter set is estimated daily. If there is less than 10 days of prior data no second volume correction is applied.

The LAWR used in this study is the Aarhus LAWR which is the primary research LAWR of DHI and the radar that has been in operation for the longest period at the same location. The location was chosen because of easy access, power, an internet connection and close proximity to the office. The drawback is that the LAWR is situated underneath a large four-legged lattice antenna mast resulting in beam blockage and partial shielding. During the 10 years it has been in operation, the surrounding trees have grown and they now interfere with the beam path in some places. By accumulating reflectivity from the months July–November 2008, the blocked sector to the west is clearly evident in Fig. 7. Fig. 7 furthermore illustrates the effect of the increasing beam resulting in decreasing accumulations with increasing range, which are equalized by the volume correction. The data in Fig. 7 has only been applied to the volume correction part of the signal processing, and in the case of the Aarhus LAWR the C_2-value was 1 and the C_3-value was −0.003. As result of the large blocked areas, the basic assumption of homogeneity used in estimation of the volume correction parameters does not hold. The second volume correction normally applied prior to the calibration is therefore not applied to the dataset used here, since the estimated C_2 and C_3 parameters would be skewed due to the large area that is blocked.

The accumulated reflectivity map of the inner 20 km in Fig. 7 furthermore illustrates that in cases such as the Aarhus LAWR where beam blockage/shielding is present, the location of gauges used for calibration and validation is crucial. Fig. 7

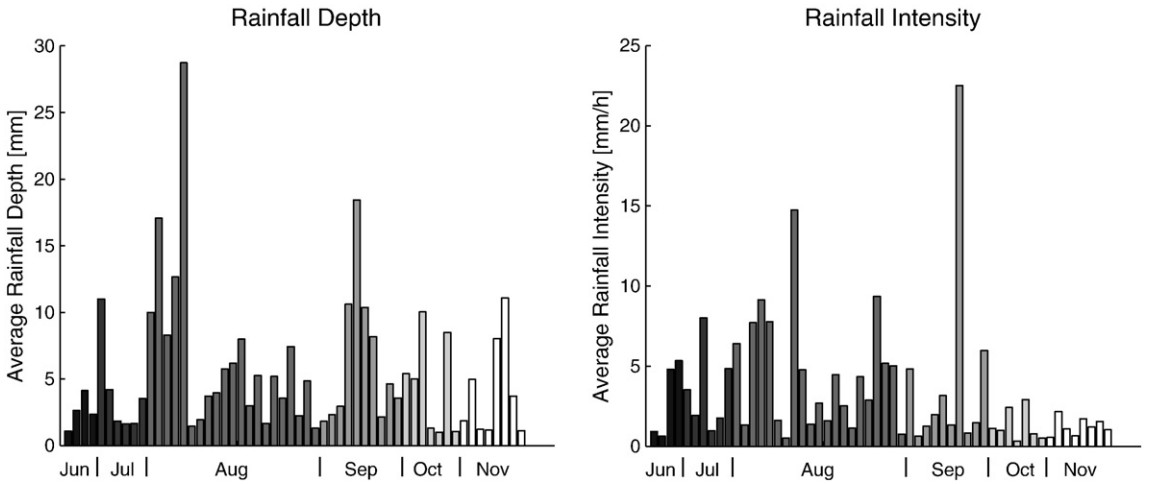

Fig. 4. Rainfall depths and rainfall intensity for all events for the gauges used in the calibration analysis (1–9). The values are an average of the gauges functioning in the particular rainfall event — from 3 to 9.

reveals that not all gauges available are equally suitable as they are placed in locations with beam shielding and thereby a general lower level of reflectivity. The gauges used for the calibration in Section 5 are located in the location marked Gauge Site in Fig. 7 which is at an unobstructed location, and so is the location of G22331. Gauges G22554 and G22361 are both located in areas affected by shielding caused by the mast.

For this specific dataset from the Aarhus LAWR, a 2D volume correction has been applied adjusting the levels of reflectivity to match those of the area with the gauges used for calibration. The accumulated reflectivity has been divided into 100 intervals linearly spaced, and the relation between a given pixel and the value of the pixel over the gauge site has been estimated. The result is a 2D image of volume correction factors ranging from a factor 0.29 to 4 — the maximum correction is limited to 4 as in the standard volume correction as shown in Fig. 8 in order to avoid over correction as a result of the correction scheme in an exponential function. The adjusted reflectivity image is shown in Fig. 9, where it can be seen that Gauges 22554 and 22321 now have the same reflectivity level, while Gauge 22361 still has a lower level.

5. Analysis of LAWR Calibration Methodology

The calibration analysis is carried out on rainfall events where both the radar and the gauges (>1 mm rainfall depth) have observed rainfall — a total of 50 rainfall events. One of the challenges is to define the appropriate time frame since the LAWR observes an area and records rainfall prior to and after the observations of the corresponding gauge. The analysis carried out here has been performed on LAWR accumulations over the timeframe defined by the gauge. This can result in underestimation of LAWR accumulations, however, when compared to extending the time frame by 10 min at the beginning and at the end of the rainfall event, in the majority of the rainfall events this is less than 5%.

The standard LAWR calibration, cf. Eq. (3) is obtained by estimating the DHI CF parameter in Eq. (4) by linear regression. The result is shown in Fig. 10.

$$Rainfall\,Depth = DHI\,CF \cdot \sum_{Event\,Start}^{Event\,Stop} Z / \Delta t, \text{where } \{\widehat{DHI\,CF} = 1.04 \cdot 10^{-3}. \quad (4)$$

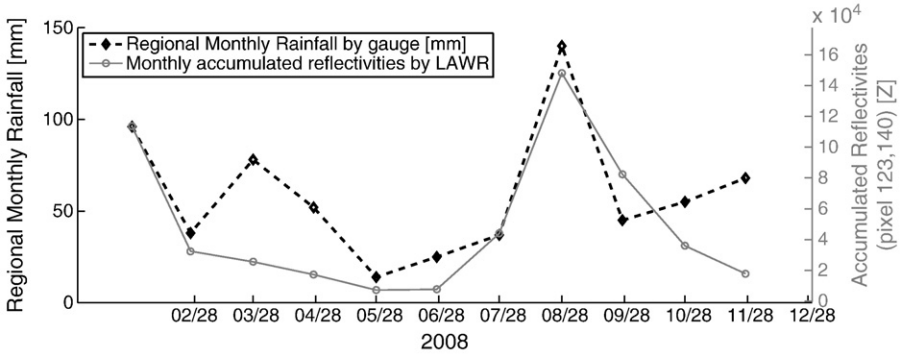

Fig. 5. Accumulated regional rainfall for the Aarhus region on monthly basis reported by DMI (2008) compared to the monthly accumulated reflectivities from pixel 123,140 (500×500 m). The marker indicating the accumulation for a given month is placed at the last day of the month (last point is 30th November).

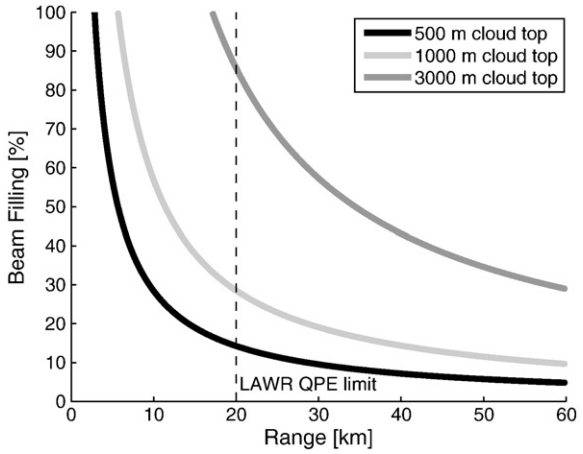

Fig. 6. Beam filling degree for three different cloud top heights as function of range with vertical angular opening of 10°. The cloud top heights are typical for nimbostratus clouds.

The estimated DHI CF of $1.04 \cdot 10^{-3}$ is used to convert Z values into rainfall intensities in mm/min — in order to get the LAWR rainfall estimates in e.g. μm/s, ordinary unit conversion is applied and the DHI CF becomes 0.007. It should be noted that some precautions must be taken when applying unit conversion since the calibration depends on the temporal resolution of the LAWR data, which can be either 1 or 5 min — here 1 min data is used.

The scatter of the data in Fig. 10 is the result of comparing a surface measurement (0.25 km^2) with a point measurement (~200 cm^2) combined with the inter-event variability of the accumulated rainfall depths observed by the gauge. The variability in rainfall depths within a 500 × 500 m area based on the 9 rain gauges was found to vary from 1 to 26% based on the coefficients of variation of the inter-event variability. The variability decreases with increasing rainfall depths and is independent of the mean rainfall event intensity (Pedersen et al., 2009). The accumulated reflectivity in Fig. 10 originates from 4 different pixels, cf. Table 2, which is clearly evident in

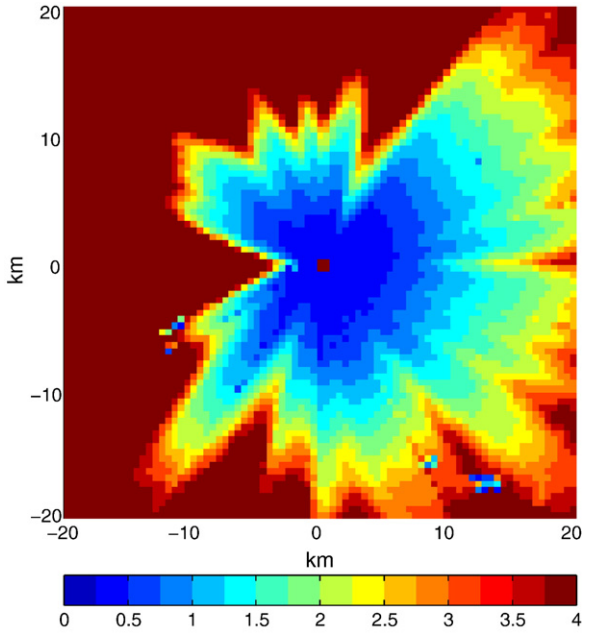

Fig. 8. 2D volume correction factors for adjusting reflectivity levels to match those of the gauge site. A maximum correction constraint of 4 is enforced.

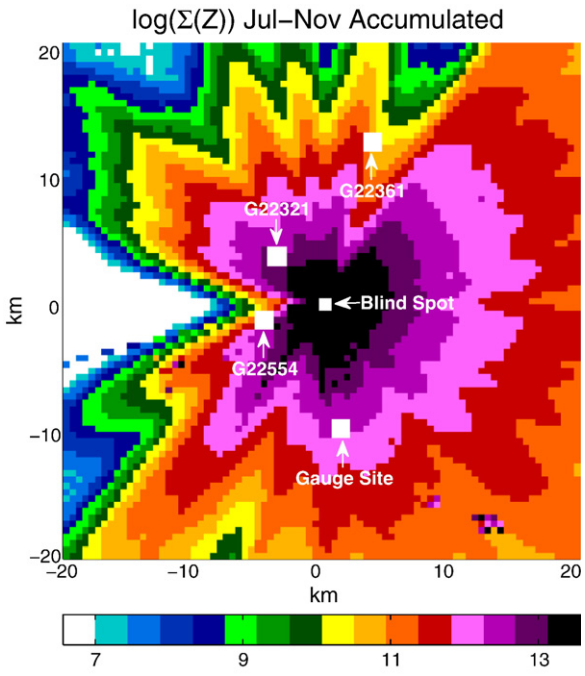

Fig. 7. Accumulation over 5 months of 2008 for 0–20 km range. Please note that the data has been log transformed for plotting.

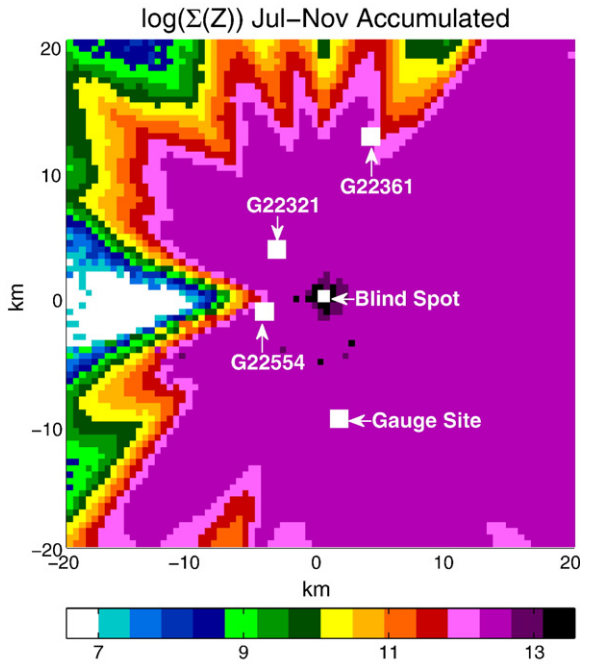

Fig. 9. Accumulated reflectivity's from the Aarhus LAWR (July–November 2008) after the 2D adjustment from Fig. 7 is applied.

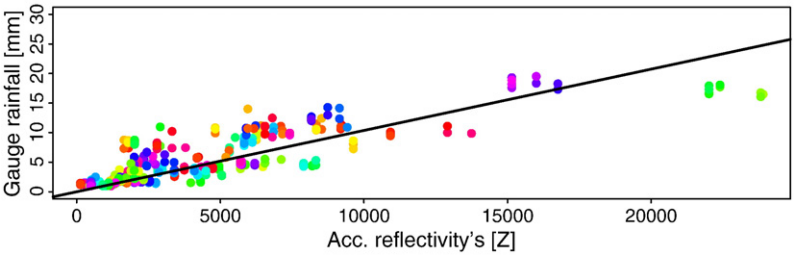

Fig. 10. Estimation of LAWR calibration factor (DHI CF) as defined by Eq. (4). Data are colored with respect to event and gauge number — same color range e.g. green for the event and different shades of green for each gauge.

the two largest rainfall events where there is a relatively large difference in the accumulated reflectivity within the same rainfall event.

It is well known that different types of rainfall have different drop size distributions resulting in different *Z–R* relationships for stratiform rainfall and convective rainfall (Battan, 1973) and others. So far there has been no attempt to use rainfall type classifications in connection with the LAWR calibration.

The standard LAWR calibration only depends on the reflectivity (*Z*), but past experience shows that the calibration factor changes significantly from rainfall events with high intensity to long lasting rainfall events with low intensities. Inspired by this and the link between different *Z–R* relationships and different rainfall types, multiple linear regression analysis is used to evaluate which variables are significant in the calibration. Initially, the full model containing all variables: acc. reflectivity (ΣZ), duration (hour), intensity (ΣZ/hour), pixel number and gauge number are estimated, after which variables with an estimated *p*-value larger than 5% are removed in order to establish the most simple model. The simplest model where all variables are significant at the 5% level contains acc. reflectivity (ΣZ), duration (hour) and intensity (ΣZ/hour). The gauge number and pixel number were found to be insignificant which indicates that the calibration is not biased towards a specific gauge or pixel. In order to determine if the simplified model is significantly poorer than the full model containing all five variables, the two models were compared by means of an ANOVA test (*F*-test). The conclusion of the test is that the simpler model with three parameters compared to the full model could not be rejected at a 1% significant level.

The estimated parameters for the chosen model:

$$\textit{Rainfall Depth} = \varphi\cdot\Sigma Z + \phi\cdot\textit{Duration} + \psi\cdot\textit{Intensity}, \qquad (5)$$

$$\text{where} \begin{cases} \hat{\varphi} = 5.96\cdot 10^{-4}[Z] \\ \hat{\phi} = 0.60 \qquad [h] \\ \hat{\psi} = 4.20\cdot 10^{-4}[Z/h] \end{cases}.$$

Table 4 summarizes the two different calibration schemes chosen for converting accumulated reflectivity into rainfall depth in mm. Scheme 1 is the standard calibration approach and Scheme 2 is the new approach as defined in Eq. (5). Duration and intensity have been removed individually from Scheme 2 and the degree of explanation is between Scheme 1 and Scheme 2.

Scheme 2 provides a better degree of explanation than Scheme 1 (standard calibration) based on the increase in *R*-squared from 0.85 to 0.90. Of the parameters in Scheme 2, reflectivity is the most significant followed by duration and finally by intensity judged by the *t*-statistic values.

5.1. Validation of extended DHI LAWR calibration

Fig. 11 shows the difference (percent) between the gauge observed rainfall depth and the LAWR estimated rainfall depth. The difference between observed and estimated rainfall is partly due to the natural scatter when comparing radar and gauge measurements and the uncertainty of the calibration method. The natural scatter contains the uncertainty related to representing the spatial variability of rainfall depths within a single LAWR pixel with a single gauge. The spatial variability expressed as coefficient of variation has in another connection been estimated from 1 to 26% for rainfall depths observed by gauge within an area corresponding to a single LAWR pixel and is marked in Fig. 11 to illustrate the part of the uncertainty which may potentially be a result of a single gauge not being representative for the whole pixel. The validation data has been applied to the 2D volume correction outlined in Section 4.2.

For all gauges there are rainfall events where the LAWR overestimates more than 100%, but in most cases of rainfall events with depths between 1 and 1.4 mm and a duration of less than 1 h. Especially light low-hanging frontal rainfall is difficult to estimate correctly by the LAWR due to the rapidly increasing beam volume. At far ranges low-hanging light rain only fills a small fraction of the LAWR sample volume, and since the rainfall estimate is an integration of the full vertical, little rain will be under the cut-off value and therefore the estimate for that point is zero.

Table 4
Summarized information on the LAWR calibration schemes. The parameters are estimated based on a total of 353 observations of 55 rain events. The figures in brackets are the standard deviation of the estimated parameter.

	Formulation	Estimated parameters	R^2
Scheme 1	Rainfall Depth = DHI CF·ΣZ	DHI CF = 1.04·10 (0.24) [*Z*]	0.85
Scheme 2	Rainfall Depth = φ·EZ + ϕ·Duration + ψ·Intensity	φ = 5.96 · 10 (0.40 · 10) [*Z*] ϕ = 0.60 (0.05) [h] ψ = 4.20 · 10 (0.48) [*Z*/h]	0.90

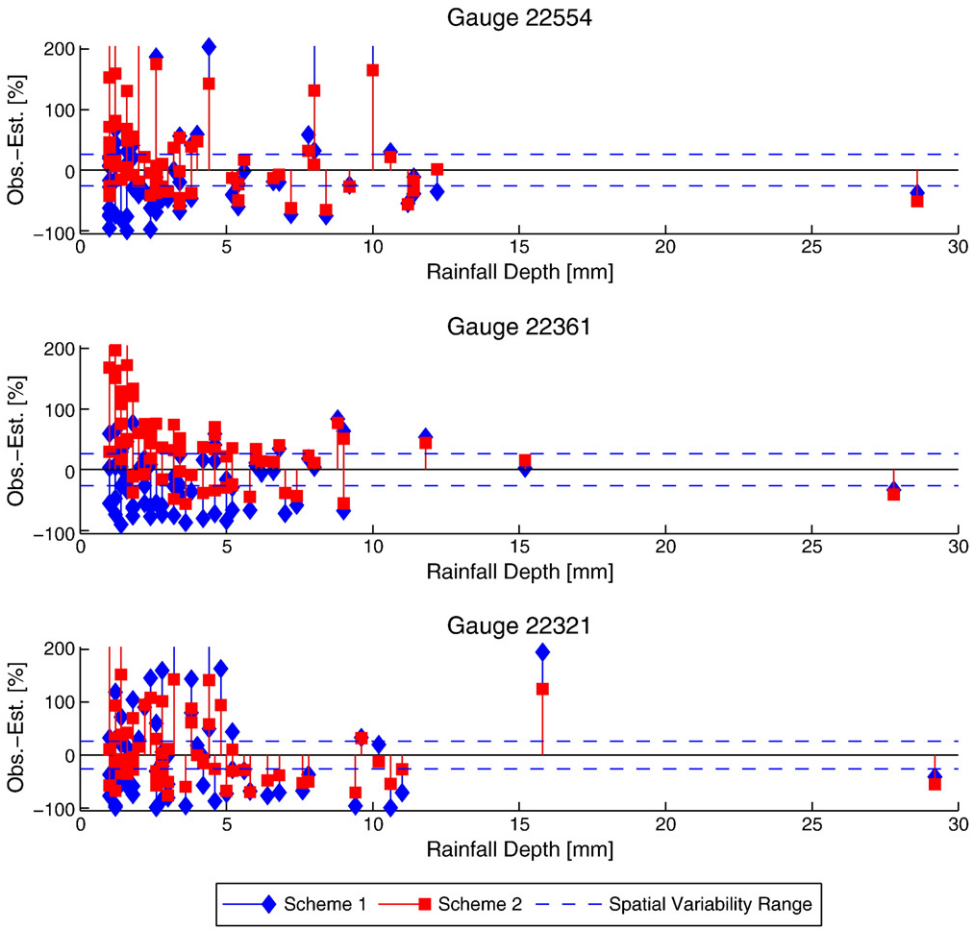

Fig. 11. Difference in percent between observed rainfall depth (mm) and LAWR estimated rainfall depth (mm) for all valid validation events for the three different gauges as function of rainfall depth. Gauge 22554 and 22361 are both approximately 5 km from the Aarhus LAWR while gauge 22321 is 13 km away. Negative percentage figures indicate the LAWR estimate is smaller than the gauge observation. The LAWR data has been applied a 2D volume correction. The spatial variability range is the maximum coefficient of variation of rainfall depths within a single LAWR pixel based on rain gauge measurements from Pedersen et al. (2010).

The two schemes are validated with 3 rain gauges operated by the Danish Meteorological Institute. Data from the corresponding LAWR pixels, cf. Table 2, is applied to the calibration schemes and the estimated rainfall depths are compared to those observed by the gauges. The location of the rain gauges in relation to the LAWR can be seen in Fig. 7. The estimated accumulations for all valid rainfall events and the observations are listed in Table 5.

Fig. 11 and the values in Table 5 show that both schemes perform very well at locations where the reflectivity level is in the same order as where the calibration factors are estimated — up to 20 km range from the radar depending on the azimuth. This condition is not fulfilled for Gauge 22361 which is located in an area with severe beam shielding, and here the 2D volume correction is insufficient. As a result of this Scheme 1 underestimates the rainfall depths (as expected from previous experience) while Scheme 2 overestimates the rainfall depths. Scheme 2 improves the calibration in 68% of the events for Gauge 22554, 36% of the events for Gauge 22361 and in 72% of the events for Gauge 22321.

The validation based on Gauge 22361 is the worst with an underestimation of −13% (Scheme 1) and an overestimation of 20% (Scheme 2). This gauge is more than twice the distance from the LAWR than the two other gauges, but this is probably of less importance than the fact that the reflectivity

Table 5
Observed and LAWR estimated rainfall depths for the three different schemes in absolute values and percent deviation from the observed rainfall depth. The percentage values in brackets are the validation based on LAWR data without 2D volume correction.

	Gauge 22554	Gauge 22361	Gauge 22321
Number of events	68	66	64
Distance to LAWR [km]	4.9	5.3	13.3
Observed total rainfall depth [mm]	280 (σ=4.4 mm)	279 (σ=4.1 mm)	270 (σ=4.3 mm)
Scheme 1 total rainfall depth [mm]	285 (σ=5.9 mm)	241 (σ=4.3 mm)	257 (σ=6.6 mm)
Scheme 2 total rainfall depth [mm]	301 (σ=4.5 mm)	334 (σ=3.8 mm)	263 (σ=4.9 mm)
Scheme 1 obs-estimated [%]	2 (−30)	−13 (57)	−5 (−76)
Scheme 2 obs-estimated [%]	7 (−11)	20 (61)	−2 (−44)

Table 6
Calibration parameters estimated based on the three validation gauges all part of the official Danish rain gauge network. The LAWR data has been applied the 2D volume correction. The figures in brackets are the standard deviation of the estimate.

	Gauge 22554	Gauge 22361	Gauge 22321
Scheme 1	DHI CF = 6.67·10 (0.74) [Z], R = 0.60	DHI CF = 9.70·10 (0.59) [Z], R = 0.81	DHI CF = 5.82·10 (0.69) [Z], R = 0.57
Scheme 2	φ = 2.09 · 10 (1.09) [Z] ϕ = 0.98 (0.23) [h] ψ = 4.74 · 10 (1.82) [Z/h] R^2 = 0.72	φ = 7.06 · 10 (1.29) [Z] ϕ = 0.27 (0.20) [h] ψ = 4.80 · 10 (1.46) [Z/h] R^2 = 0.84	φ = 2.34 · 10 (1.05) [Z] ϕ = 0.96 (0.24) [h] ψ = 0.89 · 10 (0.55) [Z/h] R^2 = 0.68

level at this point is more than 4 times lower than that of the area used for the calibration parameter estimation. The lower reflectivity level at Gauge 22321 is a combination of beam filling effects and beam shielding as a result of the antenna mast. The data foundation is too weak for any final conclusions on the range effect of the calibration. Unfortunately, the number of validation gauges available was limited to 3 at only two different distances to the LAWR. In order to establish if there is a range dependency that needs to be implemented in the calibration schemes, a higher number of gauges at increasing distances from the LAWR are required.

If the validation is carried out over an inhomogeneous reflectivity field as in Fig. 7 (without second step volume correction) the proposed new scheme has improved the LAWR calibration compared to the existing one. Both for Gauge 22554 and 22321, their estimate is in the order of twice as good as that of Scheme 1. The validation results of Gauge 22554 are the best with an average underestimation of −11% by Scheme 2. Generally, Scheme 2 outperforms Scheme 1 except for Gauge 22361, where Scheme 1 is slightly better, but both schemes overestimate the observed rainfall. The validation results without second step volume correction vary as expected when the location of the gauges relative to the accumulated reflectivity level is taken into account in Fig. 7. The log(ΣZ) value of the gauge locations are: 12.3 (Gauge 22554), 13.1 (Gauge 22361) and 11.2 (Gauge 22321). When compared to the log(ΣZ) value of 12.6 from the Gauge Site where the calibration factors are estimated, it becomes evident that the variation of the validation results is a result of the different accumulation reflectivity levels which again are an expression of the general signal level in that point. The large variation in the signal level in Fig. 7 would not be present under normal conditions, so the results would be in the same order as those obtained using the 2D volume-corrected data.

Based on the validation results it is found that both schemes perform equally well if the reflectivity levels are homogenous over the area. In situations where this is not the case the new calibration method proposed denoted Scheme 2 is better than the original calibration method (Scheme 1). Scheme 2 provides the best rainfall estimation in such cases.

The gauges used for the calibration estimation are from a temporary installation dedicated to addressing LAWR calibration uncertainties related to spatial variability of rainfall. The LAWRs in Denmark normally use data from the official Danish rain gauges network (SVK), so in order to link the findings based on the temporary gauges, the three available official gauges have been used to estimate the calibration parameters. The estimated parameters based on the official gauges are listed in Table 6 and the tendency is the same with Scheme 2 resulting in the best results. As expected there is quite large variation in the estimated parameters due to the location of the gauges in relation to the general reflectivity level. It should be stressed that it is of utmost importance to identify the location of gauges used for calibration in relation to the overall reflectivity level as done in Fig. 7 since the estimated calibration factors in principle are only valid for areas of equal reflectivity level to the calibration gauge(s).

To illustrate the LAWR's ability to estimate the rainfall, intensities from two events from Gauge 222554 have been shown in Figs. 12 and 13.

The rainfall event of 7 July (Fig. 12) illustrates the effect of measuring rainfall with gauge and with radar. The gauge records some very short lasting peak intensities which are observed differently by the radar since the LAWR intensity sample is an average over a volume and over a time span, whereas the gauge is a discrete measurement in a small point. The key issue here is the scaling properties of the rainfall since the gauge estimate is only representative for a small area whereas the radar is an average of a volume over an area. Fig. 13 shows a rainfall event where the LAWR correctly represents periods with no rain which are missed by the gauge due to the interpolation technique used, where the tip is divided by the minutes since the last tip and the mean value is used for all intermediate time steps. For both events there is good agreement of the timing between the gauge and the LAWR. The first peak (3.3 μm/s) in the gauge time series on

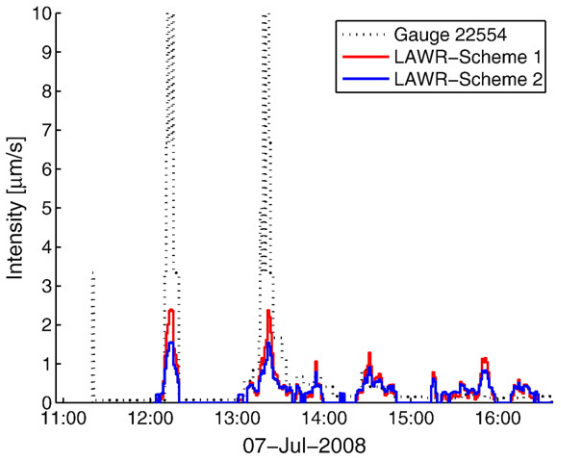

Fig. 12. Intensities observed by DMI gauge and by LAWR the 7th of July. The rainfall event has two high peak intensities lasting only 1–2 min. The rainfall depth observed by the gauge was 11.4 mm, while the LAWR estimate was 7.0 mm (Scheme 1) and 7.6 mm (Scheme 2). The LAWR data has been applied the 2D volume correction.

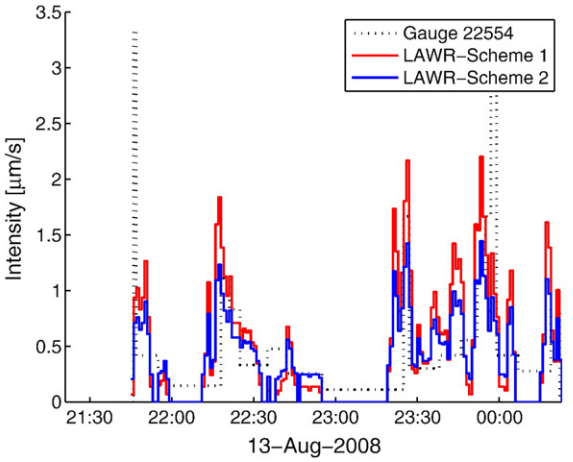

Fig. 13. Intensities observed by DMI gauge and by LAWR on the 13th of August. The rainfall event has 3 subparts which is captured by the LAWR but lost in the interpolation technique of the gauge. The rainfall depth observed by the gauge was 4.0 mm, while the LAWR estimate was 6.4 mm (Scheme 1) and 5.9 mm (Scheme 2). The LAWR data has been applied the 2D volume correction.

both plots is an artifact from the gauge data processing. Since there is no way to know the time to fill the first gauge bucket, it is fixed to 1 min and thus the significant peak.

6. Conclusions

The LAWR system and key data processing methods have been reviewed together with the existing calibration method. The focus point of the work has been to evaluate the performance of the LAWR and identify the significant factors affecting the calibration and thereby the uncertainty of the output. Based on a relatively large dataset obtained during a field campaign in 2008 where 9 rain gauges where placed within a 500×500 m area and three independent validation sets of data from the official Danish gauge network, the existing calibration method was evaluated. The existing calibration method for converting LAWR reflectivity into rainfall intensity is based on a linear relationship between the rainfall depth of a rainfall event observed by gauge and the corresponding amount of accumulated reflectivity. The linear relationship is a result of the logarithmic receiver, contrary to the linear receiver of conventional weather radars resulting in a power-law relationship between rainfall and reflectivity. The standard one parameter LAWR calibration method has been observed to generally underestimate the LAWR rainfall. It was therefore of interest to search for a new calibration method which could reduce the uncertainties of the LAWR rainfall estimation. Based on the set of data from the 9 rain gauges, a new calibration scheme was developed. As the standard LAWR calibration, it uses the assumption of linear relationship between gauge rainfall and reflectivity, but it also includes the duration and the intensity observed by the LAWR. The new scheme improves the explanation degree of the calibration compared to the standard calibration with an increase in R^2 from 0.85 to 0.9 (Scheme 2).

The validation revealed that the location of the calibration gauge(s) is extremely important since the overall reflectivity level of the Aarhus LAWR is inhomogeneous as a result of the location underneath an antenna mast causing beam blockage and shielding effects. Furthermore, growing trees result in signal absorption, and finally a hill to the west cause a large sector to be blocked. As a result of this, it was not possible to derive and apply the normal second step volume correction which aims at adjusting the reflectivity levels. Instead a 2D volume correction adjusting the reflectivity levels to match the level of the gauge site with the calibration gauges was applied to obtain homogenous conditions over the validation gauges. This method was found to result in a homogenous reflectivity field, but the method needs further development and testing before it is implemented in operational context. If the magnetron output level in the future is automatically adjusted to be constant over time, the 2D volume correction should be a constant filter, but individual for each radar.

The validation results showed very good agreement for gauges where the LAWR reflectivity level was in the same order as over the calibration gauges. If the reflectivity level is homogenous, both calibration methods perform equally well and the error is within $\pm 7\%$, while at locations affected by beam shielding, Scheme 1 results in underestimation (-13%) and Scheme 2 in overestimation ($+20\%$). At the shielded location (Gauge 22361) Scheme 1 is best in 64% of the validation events. If the reflectivity levels over the radar coverage areas are as inhomogeneous as those of the Aarhus LAWR used here (Fig. 7), the new Scheme 2 calibration method outperforms the standard calibration.

The different uncertainties contributing to the total uncertainty are dominated by the range dependent uncertainties of a non-uniform rainfall field, increasing beam volume and attenuation. The random uncertainty as a result of spatial variability of rainfall depths within a single LAWR pixel ranges from 1 to 26% confines the accuracy limit of a calibration using a single gauge despite perfect radar data. The new calibration schemes can reduce the uncertainty level of the LAWR rainfall estimate, but in order to reduce the uncertainties more, the problem with different reflectivity levels needs to be addressed. A two dimensional mask as attempted here containing the level characteristics combined with the volume characteristics could be a solution to this issue.

The LAWR bridges the domain gap between rain gauge and conventional radars and provides information at the missing scales which is central in connection with urban drainage issues. Radars reveal the spatial structure of the rainfall in real time which is not possible to obtain by a few gauges, and furthermore they can provide forecast information. By combining information from gauge networks, LAWRs and conventional radars into a joint framework, it becomes possible to reduce some of the uncertainties at the different levels. The challenge is to balance the potential gain in information level with the attached uncertainties originating from combining measurements at different spatial and temporal scales, which is also the core of comparing LAWR rainfall data with gauge data.

References

Arnbjerg-Nielsen, K., 2006. Significant climate change of extreme rainfall in Denmark. Water Science and Technology 54 (6–7), 1–8.
Austin, M., 1987. Relation between measured radar reflectivity and surface rainfall. Monthly Weather Review 115 (5), 1053–1070.

Battan, L.J., 1973. Radar Observations of the Atmosphere. The University of Chicago Press.
Bouar, E., Moreau, E., Testud, J., Poulima, H., Ney, R., Deudon, O., 2005. An extensive validation experiment of algorithm ZPHI. Proceeding from the 32nd Conference on Radar Meteorology. American Meteorological Society, Albuquerque.
Brotzge, J., Droegemeier, K., McLaughlin, D., 2006. Collaborative Adaptive Sensing of the Atmosphere (CASA): a new radar system for improving analysis and forecasting of surface weather conditions. Journal of the Transportation Research Board 1948, 145–151.
Chocat, B., Krebs, P., Marsalek, J., Rauch, W., Schilling, W., 2001. Urban drainage redefined: from stormwater removal to integrated management. Water Science and Technology 43 (5), 61–68.
Ciach, G.J., Krajewski, W.F., 1999. Radar-rain gauge comparisons under observational uncertainties. Journal of Applied Meteorology 38, 1519–1525.
DMI, 2008. Måneden, sæsonen og årets vejr. http://www.dmi.dk/dmi/index/danmark/maanedens_vejr_-_oversigt.htm2008[Online]: 15 October 2008.
Donovan, B.C., Hopf, A., Trabal, J.M., Roberts, B.J., McLaughlin, D.J., Kuros, J., 2006. Off-the-grid radar networks for quantitative precipitation estimation. Proceedings from Fourth European Conference on Radar in Meteorology and Hydrology (ERAD06), Barcelona, Spain.
Doviak, R.J., Zrnic, D.S., 2006. Doppler Radar and Weather Observations, 2 Edition. Dover Publications.
Einfalt, T., Jessen, M., Mehlig, B., 2005. Comparison of radar and raingauge measurements during heavy rainfall. Water Science and Technology 51 (2), 195–201.
Fiser, O., 2004. Z–R (Radar Reflectivity–Rain rate) relationships derived from Czech Distrometer data. Proceedings from Third European Conference on Radar in Meteorology and Hydrology (ERAD04), Visby, Sweden.
Gekat, F., Pool, M., Didszun, J., 2008. Performance comparison of a compact weather radar featuring different antennas. Proceedings of the Fifth European Conference on Radar in Meteorology and Hydrology (ERAD08), Helsinki, Finland.
Grum, M., Jørgensen, A.T., Johansen, R.M., Linde, J.J., 2006. The effect of climate change on urban drainage: an evaluation based on regional climate model simulations. Water Science and Technology 54 (6–4), 9–15.
Habib, E., Krajewski, W.F., 2001. Uncertainty analysis of the TRMM ground-validation radar-rainfall products: application to the TEFLUN-B Field campaign. Journal of Applied Meteorology 41, 558–572.
Jameson, A.R., Kostinski, A.B., 2001. Reconsideration of the physical and empirical origins of Z–R relations in radar meteorology. Quarterly Journal of the Royal Meteorological Society 127 (517), 517–538.
Jensen, N.E., 2002. X-Band local area weather radar — preliminary calibration results. Water Science and Technology 45 (2), 135–138.
Jensen, N.E., Pedersen, L., 2005. Spatial variability of rainfall. Variations within a single radar pixel. Atmospheric Research 77, 269–277.
Krajewski, W.F., Ciach, G.J., Habib, E., 2003. An analysis of small-scale rainfall variability in different climate regimes. Hydrological Sciences Journal 48 (2), 151–162.
Lee, G., Zawadzki, I., 2004. Errors in rain measurements by radar due to variability of drop size distributions. Proceedings of Sixth International Symposium on Hydrological Applications of Weather Radar, Melbourne, Australia.
Lee, G., Zawadzki, I., 2005. Variability of drop size distributions: time-scale dependence of the variability and its effects on rain estimation. Journal of Applied Meteorology 44 (2), 241–255.
Lee, G., Seed, A.W., Zawadzki, I., 2007. Modeling the variability of drop size distributions in space and time. Journal of Climate and Applied Meteorology 46 (6), 742–756.
Mailhot, A., Duchesne, S., Caya, D., Talbot, G., 2007. Assessment of future change in intensity — duration–frequency (IDF) curves for Southern Quebec using the Canadian Regional Climate Model (CRCM). Journal of Hydrology 347, 197–210.
Marshall, J.S., Palmer, W.M., 1948. The distribution of raindrops with size. Journal of Meteorology 5, 165–166.
Marshall, J.S., Langille, R.C., Palmer, W.M., 1947. Measurements of rainfall by radar. Journal of the Atmospheric Sciences 4 (6), 186–192.
Overgaard, S., 2001. Preliminary evaluation of the FUENEN LAWR WEATHER RADAR. Technical Note, Danish Meteorological Institute.
Pedersen, L., 2004. Scaling Properties of Precipitation — experimental study using weather radar and rain gauges. M.Sc. Thesis. Aalborg University.
Pedersen, L., Jensen, N.E., Christensen, L.E., Madsen, H., 2010. Quantification of the spatial variability of rainfall based on a dense network of rain gauges. Journal of Atmospheric Research 95 (4), 441–454.
Rinehart, R.E., 2004. Radar for Meteorologists, 4. Rinehart Publications.
Thomsen, R.S., 2007. Drift af Spildevandskomitéens Regnmålersystem Årsnotat. Teknisk rapport 08-06. Danish Meteorological Institute (in Danish).
Uijlenhoet, R., 2001. Raindrop size distributions and radar reflectivity–rain rate relationships for radar hydrology. Hydrology and Earth System Sciences 5 (4), 615–627.
Uijlenhoet, R., Porra, J.M., Sempere Torres, D., Creutin, J.-D., 2008. Analytical solutions to sampling effects in drop size distribution measurements during stationary rainfall: Estimation of bulk rainfall variables. Journal of Hydrology 328, 65–82.
Ulbrich, W.C., 1983. Natural variations in the analytical form of the raindrop size distribution. Journal of Climate and Applied Meteorology 22, 1764–1775.
Zawadzki, I., 1974. On radar–raingauge comparison. Journal of Applied Meteorology 14 (1430), 1436.
Zawadzki, I., 1984. Factors affecting the precision of radar measurements of rain. Proceedings of 22nd Conference on Radar Meteorology. The American Meteorological Society.